



Pacific meridional mode and El Niño—Southern Oscillation

Ping Chang,¹ Li Zhang,² R. Saravanan,³ Daniel J. Vimont,⁴ John C. H. Chiang,⁵ Link Ji,¹ Howard Seidel,¹ and Michael K. Tippett⁶

Received 6 April 2007; revised 21 June 2007; accepted 31 July 2007; published 30 August 2007.

[1] We present intriguing evidence that the majority of El Niño events over the past four decades are preceded by a distinctive sea-surface warming and southwesterly wind anomaly in the vicinity of the Intertropical Convergence Zone (ITCZ) during the boreal spring. This phenomenon, known as the Meridional Mode (MM), is shown to be intrinsic to the thermodynamic coupling between the atmosphere and ocean. The MM effectively acts as a *conduit* through which the extratropical atmosphere influences ENSO. Modeling results further suggest that the MM plays a vital role in the seasonal phase-locking behavior of ENSO. The findings provide a new perspective for understanding the important role of thermodynamic ocean-atmosphere feedback in ENSO and may have profound implications for ENSO prediction, particularly the unresolved issue of the spring predictability barrier.

Citation: Chang, P., L. Zhang, R. Saravanan, D. J. Vimont, J. C. H. Chiang, L. Ji, H. Seidel, and M. K. Tippett (2007), Pacific meridional mode and El Niño—Southern Oscillation, *Geophys. Res. Lett.*, 34, L16608, doi:10.1029/2007GL030302.

1. Introduction

[2] Recent studies have linked the onset of ENSO to extratropical atmospheric variability [Vimont *et al.*, 2003; Pierce *et al.*, 2001], which in contrast to the tropics is, to a large extent, driven by the internal dynamics of the atmosphere [Saravanan, 1998; Kushnir *et al.*, 2002]. The dominant modes of extratropical atmospheric variability manifest themselves as large-scale sea-level pressure oscillations. Well-known examples are the North Atlantic Oscillation (NAO) [Hurrell *et al.*, 2001] and the North Pacific Oscillation (NPO) [Rogers, 1981]. The fluctuating intensity of the semi-permanent subtropical high pressure system induced by these modes of variability effectively modulates the strength of the northeasterly trade winds in the tropical latitudes, leaving an imprint on SST via changes in wind-induced latent heat flux [Vimont *et al.*,

2003]. Because the NAO and NPO modes of variability have peak variability during the boreal winter, their corresponding subtropical SST anomaly patterns (which, to first order, reflect the integrated forcing from the atmosphere) tend to have maximum variance in boreal spring.

[3] Of particular importance to this extratropical-induced SST anomaly is the anomalous north-south gradient which develops along its southern front during the following boreal spring. Studies in both the Pacific [Vimont *et al.*, 2003] and Atlantic [Hastenrath and Heller, 1977] have suggested that this SST gradient, once formed, can displace the ITCZ, which can in turn feed back onto the SST gradient through changes in the winds which modify local heat fluxes, giving rise to a co-varying pattern between the ITCZ and the north-south SST gradient in both the tropical Atlantic [Chang *et al.*, 1997] and Pacific [Chiang and Vimont, 2004]. Because of its association with the north-south SST gradient and the meridional fluctuation of the ITCZ, it has been referred to as the MM of variability [Chiang and Vimont, 2004].

2. Relationship Between MM and ENSO

[4] The boreal spring MM in Figure 1a, obtained via a Maximum Covariance Analysis (MCA) of the March–April–May (MAM) wind stress and SST anomalies that are not preceded by an ENSO event, reveals a north-south variation in winds and SST that is distinctively different from ENSO. The wind stress and SST anomalies are based on the re-analysis product, ERA-40, of the European Centre for Medium-Range Weather Forecasts (ECMWF) [Uppala *et al.*, 2005] and the Reynolds Optimum Interpolation (OI) SST [Reynolds and Smith, 1994] from 1958 to 2000, respectively. The temporal variation of the MM is characterized by two monthly time series obtained by projecting the monthly anomalies onto the MCA (Figure 1a) and is referred to as the MM wind-stress index and MM SST index. The wind index displays maximum variance during the boreal spring (Figure 1b), confirming that the MM is indeed a boreal spring phenomenon. The lag-correlation between the wind and SST indices shows a maximum value of 0.7, when the wind index leads the SST by one month, and its structure is indicative of coupled ocean-atmosphere feedbacks (Figure 1c).

[5] To reveal the relationship between the MM and ENSO, we used the MM monthly wind index averaged from January to May (JFMAM) when the MM is most active (blue in Figure 1d) and the following November–December–January (NDJ) cold tongue index (CTI) (red in Figure 1d) which is an SST based index commonly used to gauge the variability of ENSO. The correlation between the

¹Department of Oceanography, Texas A&M University, College Station, Texas, USA.

²Division of Ocean Sciences, National Science Foundation, Arlington, Virginia, USA.

³Department of Atmospheric Sciences, Texas A&M University, College Station, Texas, USA.

⁴Department of Atmospheric and Oceanic Sciences, University of Wisconsin, Madison, Wisconsin, USA.

⁵Department of Geography, University of California, Berkeley, California, USA.

⁶International Research Institute for Climate and Society, Columbia University, Palisades, New York, USA.

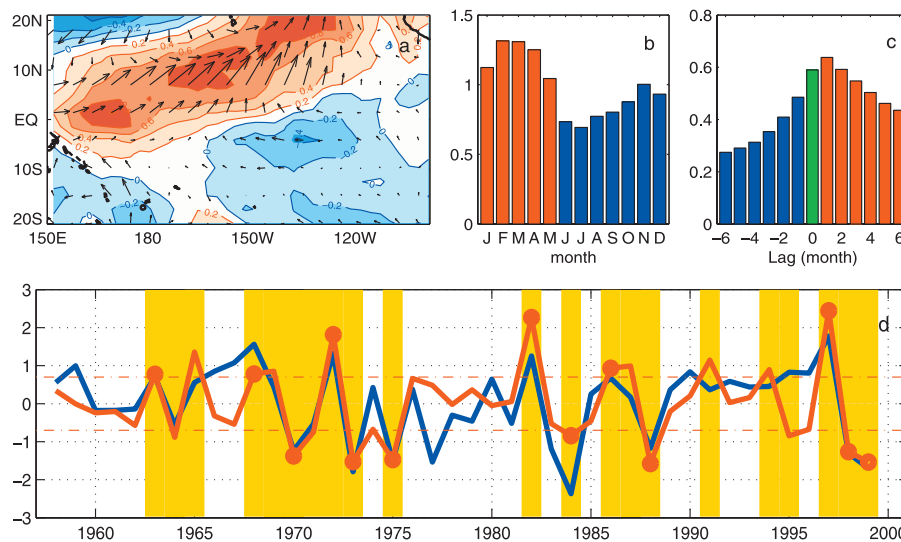


Figure 1. Observed MM and its relationship to ENSO. (a) Leading MCA pattern of the MM in non-ENSO boreal spring. Color shading indicates SST anomaly (red is positive) and the vector indicates wind anomaly. (b) Standard deviation of the monthly MM wind index as a function of calendar month. (c) Lag-correlation between the monthly wind and SST MM indices. (d) The FMAM MM wind index (blue) and the NDJ CTI (red). The horizontal dashed lines indicate 70% of the standard deviation of the indices which is used to define ENSO and MM events. The vertical shading indicates the springs that follow an ENSO event. The red dots indicate those ENSO events that are preceded by a MM event.

two time series is 0.68. Defining a MM event as episodes where the JFMAM MM wind index exceeds 70% of its standard deviation, more than 70% (12 out of 17) of the ENSO events during the past four decades are preceded by MM events. These statistical results of the MM-ENSO relationship are more robust than those of the MJO-ENSO relationship reported previously [Slingo *et al.*, 1999; Hendon *et al.*, 1999].

[6] Interestingly, there is a marked similarity between the SST pattern of the MM and the SST composite preceding the westerly wind events (WWEs) that lead to rapid ENSO development [Vecchi and Harrison, 2000], raising the possibility that the MM and WWEs may be connected. Further analysis of this linkage is, however, beyond the scope of this study. Finally, we note that the SST pattern of the MM reported here also bears a close resemblance to the optimal initial condition that leads to rapid development of ENSO [Penland and Sardeshmukh, 1995].

[7] A lag-correlation analysis between upper ocean heat content (HC) derived from an ocean data assimilation product [Carton *et al.*, 2000] and the CTI supports the finding that the MM variability leads the development of ENSO. The HC anomaly in the central equatorial Pacific is significantly correlated with the CTI when the former leads the latter by one to two months. However, similar correlation is found between the HC and the MM index when the MM leads the HC by one season. If the MM's influence on HC is removed by a linear regression, the correlation between HC and CTI is considerably weakened to a statistically insignificant level (not shown), suggesting that the role of subsurface ocean variability is to connect the MM induced wind variability to cold tongue SST variability

via equatorially trapped wave propagation [Vimont *et al.*, 2003].

3. Coupled Model Experiments

[8] To further test these findings, we conducted a series of coupled climate model experiments with the NCAR Community Climate Model version 3 (CCM3) coupled to an extended 1.5 layer reduced gravity ocean (RGO) model that has been used extensively in the study of ENSO [Zebiak and Cane, 1987]. Figure 2 illustrates the CCM3-RGO model's ability to simulate observed ENSO variability based on a 400-year coupled simulation. Many salient features of observed ENSO are reproduced, including its temporal (Figures 2a and 2b) and spatial (Figures 2f and 2g) structures, as well as its phase-locking to the seasonal cycle (Figures 2c and 2d). The coupled model does, however, underestimate ENSO variability strength by about 20% and its period by about 6 months (Figure 2e).

[9] The CCM3-RGO model also captures the boreal spring MM variability and its relation to ENSO. Figure 3a shows the leading pattern of a similar analysis applied to the simulated winds and SST. The resemblance between the observed (Figure 1a) and simulated MM is evident, except that the center of the model SST variability is shifted toward the eastern equatorial region. As in the observations, there is a robust relationship between the MM and ENSO in the model. The correlation between the JFMAM MM wind index and the NDJ CTI index in the model (not shown) is higher than 0.5 for the 400-year record, which is significant above the 99% level. Using the same ENSO and MM event definition as in the observational analysis, we found that about 66% of the simulated El Niño events are preceded by

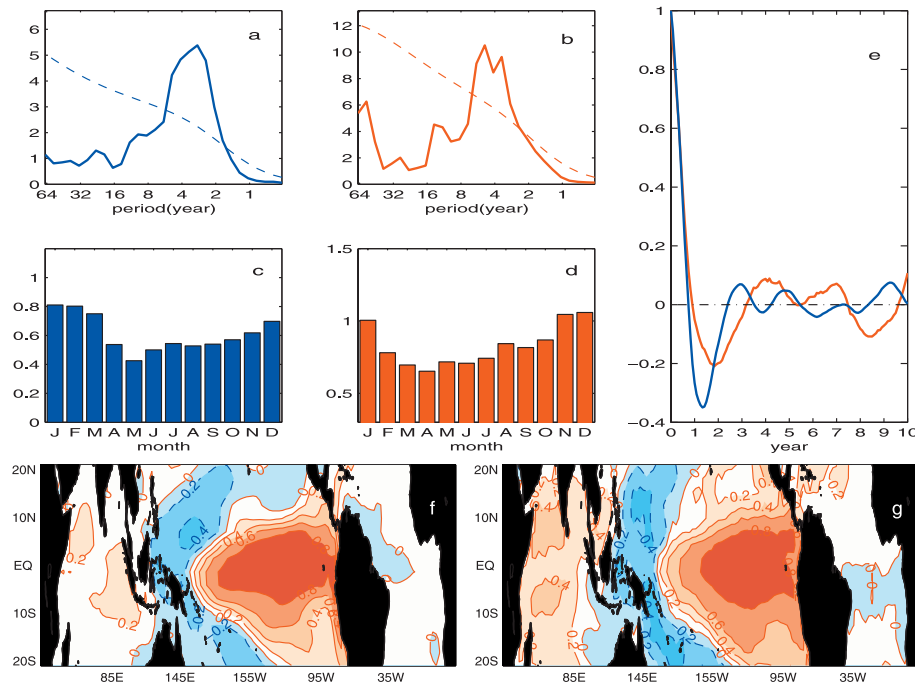


Figure 2. Comparison between observed and simulated ENSO. (a) Power spectrum of the 400-year monthly NINO3 SST index from the CCM3-RGO model simulation. (b) Same as in Figure 2a except for Kaplan SST anomaly from 1900–2000 provided by the NOAA-CIRES Climate Diagnostic Center; http://www.cdc.noaa.gov/cdc/data.kaplan_sst.html. (c) Standard deviation of the modeled NINO3 SST as a function of calendar months. (d) Same as in Figure 2c except for observed SST. (e) NINO3 SST auto-correlation for the model (blue) and observation (red). (f) Correlation of the simulated tropical SSTs with the simulated NINO3 index. (g) Same as in Figure 2f except for observed SST.

like-signed MM events. The remaining El Niños are preceded by strong westward propagating thermocline anomalies off the equator (not shown). This feature, which appears absent in the MM induced El Niños (not shown), is more in line with the delayed oscillator theory of ENSO [Suarez and Schopf, 1988; Battisti, 1988] where subsurface ocean preconditioning is crucial for the development of an ENSO event.

[10] Additional experiments using CCM3 coupled to a thermodynamics-only mixed layer ocean and with a specified observed annual cycle of SST (hereafter CCM3-ML and CCM3-AC, respectively) were carried out to demonstrate that the MM can be reproduced when ENSO is absent

in the coupled model, thereby confirming that the MM is indeed a physical entity in its own right and not a statistical artifact. These experiments also show that the observed structure and persistence of the MM are successfully captured by the CCM3-ML but not the CCM3-AC simulations (not shown), suggesting that the MM is inherent to the thermodynamic coupling between the atmosphere and ocean. Further experiments involving forcing the ocean model with the surface wind stresses and heat fluxes from the CCM3-ML run show that these forcing fields not only generate an ENSO-like response with realistic seasonal phase-locking (not shown), but also that the ENSO-like variability is significantly correlated with the MM variabil-

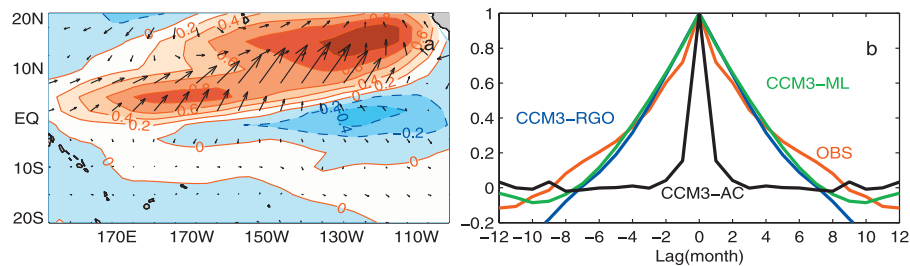


Figure 3. MM in coupled simulations. (a) Leading MCA of the non-ENSO boreal spring winds and SST from the 400-year coupled simulation of the CCM3-RGO model. (b) Auto-correlation functions of the time series obtained by projecting the monthly meridional wind stress anomalies in observation (red), CCM3-RGO simulation (blue), CCM3-ML simulation (green) and CCM3-AC simulation (black) onto the corresponding leading EOF of the boreal spring meridional wind stress anomaly.

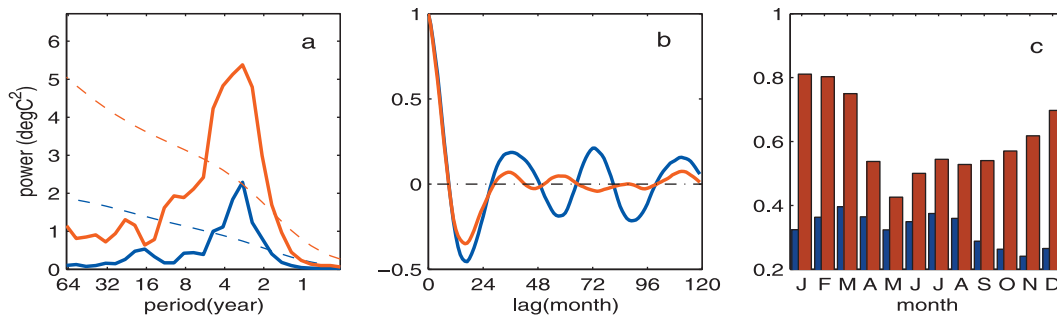


Figure 4. Effect of atmospheric noise on ENSO. (a) Power spectra, (b) auto-correlation function of the NINO3 time series, and (c) standard deviation as a function of calendar month of the simulated NINO3 time series from the filtered (blue) and unfiltered (red) coupled CCM3-RGO experiments.

ity in the CCM3-ML run with correlations exceeding 0.5 for the 100-year record. Roughly 70% of the ENSO-like events are preceded by MM events. In contrast, using the CCM3-AC fluxes to force the ocean model did not produce any ENSO-like response (not shown). These results argue strongly that the relation between the MM and ENSO derived from the observations and the CCM3-RGO simulation is statistically robust and the MM can act as a trigger of ENSO. These findings, however, should not be interpreted to mean that the Bjerknes feedback and the oceanic adjustment are not important for ENSO. In fact, they suggest the opposite. Without these processes, the ENSO-like variability in the CCM3-ML experiments does not possess the same temporal characteristics of the ENSOs in the coupled CCM3-RGO simulation, indicating that these processes are crucial in determining the intrinsic time scale of ENSO.

4. Summary and Discussion

[11] Linking MM to ENSO may shed light on unresolved issues in ENSO dynamics, such as the seasonality of ENSO: the strong seasonality of the MM suggests that it may contribute to the seasonal phase-locking of ENSO. Indeed, when the internal atmospheric variability was suppressed by the use of a “noise filter” that is composed of a series of signal-to-noise optimals [Venzke *et al.*, 1999], ranked in decreasing order of the ratio of the projected variance of the forced atmospheric response to SST to that of the internal atmospheric variability, not only is the simulated ENSO substantially weakened (Figure 4a), but it was no longer phase-locked to the boreal winter (Figure 4c). Interestingly, the periodicity of the ENSO was not affected by the weakened noise (Figure 4b). Hence, ENSO’s time scale is intrinsic to the dynamical coupled system of the tropical Pacific [Neelin *et al.*, 1998], but its phasing may be dictated by the extratropical atmospheric variability via the MM.

[12] Given that the MM activity peaks during the boreal spring, and potentially affects the onset of ENSO and its seasonal phase-locking behavior, one may conjecture that improving model skills in simulating and predicting the MM may lead to improved skill in forecasting ENSO, and ultimately eliminate the spring predictability barrier [Latif *et al.*, 1998]. If this conjecture is proven true, then a better understanding of thermodynamic feedbacks and the interaction between the tropics and extratropics in the climate

system should be considered as a high priority in future climate modeling studies.

[13] **Acknowledgments.** This work is supported through NSF grant ATM-99007625 and NOAA grant NA16GP1572.

References

- Battisti, D. S. (1988), Dynamics and thermodynamics of a warming event in a coupled tropical atmosphere-ocean model, *J. Atmos. Sci.*, *45*, 2889–2919.
- Carton, J. A., G. Chepurin, and X. Gao (2000), A simple ocean data assimilation analysis of the global upper ocean 1950–95. part II: Results, *J. Phys. Oceanogr.*, *30*, 311–326.
- Chang, P., L. Ji, and H. Li (1997), A decadal climate variation in the tropical Atlantic Ocean from thermodynamic air-sea interactions, *Nature*, *385*, 516–518.
- Chiang, J. C. H., and D. J. Vimont (2004), Analogous Pacific and Atlantic meridional modes of tropical atmosphere-ocean variability, *J. Clim.*, *17*, 4143–4158.
- Hastenrath, S., and L. Heller (1977), Dynamics of climate hazards in north-east Brazil, *Q. J. R. Meteorol. Soc.*, *103*, 77–92.
- Hendon, H., H. C. Zhang, and J. D. Glick (1999), Interannual variability of the Madden-Julian oscillation during austral summer, *J. Clim.*, *12*, 2538–2550.
- Hurrell, J. W., Y. Kushnir, and M. Visbeck (2001), The North Atlantic Oscillation, *Science*, *291*, 603–605.
- Kushnir, Y., W. A. Robinson, I. Bladé, N. M. J. Hall, S. Peng, and R. Sutton (2002), Atmospheric GCM response to extratropical SST anomalies: Synthesis and evaluation, *J. Clim.*, *15*, 2233–2256.
- Latif, M., D. Anderson, T. Barnett, M. Cane, R. Kleeman, A. Leetmaa, J. O’Brien, A. Rosati, and E. Schneider (1998), A review of the predictability and prediction of ENSO, *J. Geophys. Res.*, *103*, 14,375–14,393.
- Neelin, J. D., D. S. Battisti, A. C. Hirst, F.-F. Jin, Y. Wakata, T. Yamagata, and S. E. Zebiak (1998), ENSO theory, *J. Geophys. Res.*, *103*, 14,261–14,290.
- Penland, C., and P. D. Sardeshmukh (1995), The optimal growth of tropical sea surface temperature anomalies, *J. Clim.*, *8*, 1999–2024.
- Pierce, D. W., T. P. Barnett, N. Schneider, R. Saravanan, D. Dommenget, and M. Latif (2001), The role of ocean dynamics in producing decadal climate variability in the North Pacific, *Clim. Dyn.*, *18*, 51–70.
- Reynolds, R. W., and T. M. Smith (1994), Improved global sea surface temperature analysis using optimal interpolation, *J. Clim.*, *7*, 929–948.
- Rogers, J. C. (1981), The North Pacific Oscillation, *J. Climatol.*, *1*, 39–57.
- Saravanan, R. (1998), Atmospheric low-frequency variability and its relationship to midlatitude SST variability: Studies using the NCAR climate system model, *J. Clim.*, *11*, 1386–1404.
- Slingo, J. M., D. P. Rowell, K. R. Sperber, and F. Nortley (1999), On the predictability of the interannual behavior of the Madden-Julian oscillation and its relationship with El Niño, *Q. J. R. Meteorol. Soc.*, *125*, 583–609.
- Suarez, M. J., and P. S. Schopf (1988), A delayed action oscillator for ENSO, *J. Atmos. Sci.*, *45*, 3283–3287.
- Uppala, S. M., et al. (2005), The ERA-40 re-analysis, *Q. J. R. Meteorol. Soc.*, *131*, 2961–3012, doi:10.1256/qj.04.176.
- Vecchi, G., and D. Harrison (2000), Tropical Pacific sea surface temperature anomalies, El Niño, and equatorial westerly wind events, *J. Clim.*, *13*, 1814–1830.

- Venzke, S., M. R. Allen, R. T. Sutton, and D. P. Rowell (1999), The atmospheric response over the north Atlantic to decadal changes in sea surface temperature, *J. Clim.*, *12*, 2562–2584.
- Vimont, D. J., J. M. Wallace, and D. S. Battisti (2003), The seasonal footprinting mechanism in the Pacific: Implications for ENSO, *J. Clim.*, *16*, 2668–2675.
- Zebiak, S. E., and M. A. Cane (1987), A model El Niño–Southern Oscillation, *Mon. Weather Rev.*, *115*, 2262–2278.
-
- P. Chang, L. Ji, and H. Seidel, Department of Oceanography, Texas A&M University, College Station, TX 77843, USA. (ping@ocean.tamu.edu; link@pod.tamu.edu; hank@tamu.edu)
- J. C. H. Chiang, Department of Geography, University of California, Berkeley, CA 94720-4740, USA. (jchiang@atmos.berkeley.edu)
- R. Saravanan, Department of Atmospheric Sciences, Texas A&M University, College Station, TX 77843, USA. (sarava@tamu.edu)
- M. K. Tippett, International Research Institute for Climate and Society, Columbia University, Palisades, NY 10964-8000, USA. (tippett@iri.columbia.edu)
- D. J. Vimont, Department of Atmospheric and Oceanic Sciences, University of Wisconsin, Madison, WI 53706, USA. (dvimont@wisc.edu)
- L. Zhang, Division of Ocean Sciences, National Science Foundation, 4201 Wilson Blvd., Suite 725, Arlington, VA 22230, USA. (lzhang@nsf.gov)